Vol. 84: 15–29, 2020
https://doi.org/10.3354/ame01922

AQUATIC MICROBIAL ECOLOGY
Aquat Microb Ecol

Published online January 16

Winter river plumes shape community composition and activity of heterotrophic microorganisms on the Oregon Coast

B. Kieft[1,*], B. C. Crump[2], A. E. White[3], M. A. Goñi[2], R. S. Mueller[1]

[1]Department of Microbiology, Oregon State University, Corvallis, Oregon 97331, USA
[2]College of Earth, Ocean, and Atmospheric Sciences, Oregon State University, Corvallis, Oregon 97331, USA
[3]Department of Oceanography, University of Hawai'i at Manoa, Honolulu, Hawaii 96822, USA

ABSTRACT: Rivers and estuaries along the central Oregon margin transport large amounts of fluvial- and terrestrial-derived materials into the coastal ocean during the winter season, which can become trapped in a nearshore coastal current by local density gradients and wind forcing. The influence of these substantial and persistent allochthonous inputs on wintertime biological activity in the Oregon coastal region is not well understood. We compared prokaryotic communities inside and outside of 2 buoyant coastal river plumes off the central Oregon coast in order to understand the relationship between plume conditions and the distributions of prokaryotic populations that form the base of the wintertime coastal food web by transforming carbon and nitrogen compounds. Both free-living and particle-associated communities inside nearshore plume zones were significantly different from communities outside the plume influence. Particulate organic matter concentrations correlated with the distribution of several *Bacteroidetes* populations with established roles in complex organic matter degradation in coastal ecosystems. Plume conditions also correlated with marine *Gammaproteobacteria* that are known to degrade terrestrially derived material. Peak heterotrophic respiration rates across sampling stations occurred at a local plume particle maximum, suggesting that particulate resources transported to coastal ocean waters by river plumes may be used or transformed by co-localized heterotrophic microorganisms. Taken together, the associations between river plume resources and prokaryotic populations implicated in organic matter turnover suggest that microbes in Oregon coastal ecosystems use allochthonous resources that are transported into the coastal ocean during winter, and that these resources help shape the coastal food web during the winter season.

KEY WORDS: 16S rDNA · Coastal carbon · Coastal ocean · Coastal plume · Community composition · Free-living bacteria · Particle-attached bacteria

1. INTRODUCTION

Transformation of carbon and nutrients by microorganisms in marine coastal zones represents a substantial component of global elemental cycling (Bauer et al. 2013). Our understanding of these ecosystems is primarily derived from processes occurring when seasonally driven factors, such as wind-driven upwelling, autochthonous primary production, and nutrient fixation, are relatively high (González et al. 2003, Vargas et al. 2007, Montero et al. 2007, Nieblas et al. 2009, Checkley & Barth 2009, Sowell et al. 2011). Yet in many coastal ecosystems, there is marked seasonality in physical oceanographic processes (e.g. upwelling/downwelling, wind properties, currents) and biogeochemical conditions (e.g. nutrient concentration and source, dissolved oxygen), particularly in temperate eastern boundary regions (Capone & Hutchins 2013). Recent studies have revealed that a significant portion of annual resource inputs to these highly productive coastal zones occurs during non-upwelling conditions, highlighting the need to understand ecosystem func-

*Corresponding author: kieft1bp@gmail.com

tion at these times and to better constrain seasonal estimates of marine elemental cycling (Evans et al. 2011, Hastings et al. 2012, Saldías et al. 2012, Goñi et al. 2013, Horner-Devine et al. 2015).

River plumes transport large amounts of organic carbon and nutrients into coastal zones during periods of peak discharge, which in many locations of the Northern Hemisphere occur during the winter and spring months. Plumes form when overland rainfall or snow melt events lead to river flooding and delivery of buoyant freshwater and terrestrially derived solutes and particles to the coastal ocean. Previous work, mostly in large temperate and Arctic rivers, suggests that plumes and their associated allochthonous resources may be important sources of organic carbon and nutrients supporting coastal food web activity during periods of otherwise low autochthonous primary production (Pakulski et al. 2000, Trousellier et al. 2002, Stedmon et al. 2007, Guenet et al. 2010, Smith et al. 2010), acting as potential hotspots of sulfur cycling (Satinsky et al. 2014a), nitrification (Pakulski et al. 1995), and carbon flux (Cai 2003).

There are many coastal streams and small rivers along the Oregon margin that display peak discharges during the rainy winter months when downwelling-favorable conditions otherwise limit autochthonous phytoplankton productivity in the coastal zone. The flow of freshwater from these rivers delivers significant amounts of terrestrially derived organic carbon and nutrients to the ocean during short periods (a few days) of winter storms along the steep coastal topography (Wetz et al. 2006, Goñi et al. 2013). It is estimated that the mass of iron transported to the shelf slope by winter river plumes in this region is sufficient to sustain the entirety of summer phytoplankton primary productivity via subsequent upwelling transport (Wetz et al. 2006, Chase et al. 2007). Similarly, >90% of the annual load of dissolved inorganic nitrogen and silica entering the Oregon shelf from the Yaquina River is transported between November and April (Sigleo & Frick 2007, Brown & Ozretich 2009), and >90% of total annual organic carbon flux from the nearby Umpqua River occurs during just a few large winter storm events each year (Goñi et al. 2013). By examining plume-derived resources during their transit into the Oregon coastal zone and their association with native microbial communities, we aimed to shed light on the understudied cycling of land-derived carbon and nutrient cycles occurring in this and similar coastal ecosystems around the world.

Microbial food webs are one of the principal drivers of resource cycling and transformation in the marine environment (Fenchel 2008, and references therein). Although strong seasonality in both the composition and function of coastal microbial communities is well documented (Alonso-Sáez & Gasol 2007, Ghiglione & Murray 2012, Fortunato et al. 2012), microorganisms on the Oregon coast have been studied in several contexts primarily during the summer upwelling season (e.g. Woebken et al. 2007, Sowell et al. 2011, Smith et al. 2013), but rarely during the winter. In particular, no observations have been made to assess the relationship between river-plume-induced gradients of resources and physical conditions with prokaryote community composition and activity on the Oregon coast.

We hypothesized that river plumes can structure prokaryotic community composition and diversity due to the selection of populations with differing ecological strategies and environmental niches across contemporaneous resource and biogeochemical gradients. Specifically, we set out to test whether allochthonous plume-derived resource gradients could be linked with abundances of certain coastal heterotrophic prokaryotic populations, implicating their involvement in the turnover of plume resources during the understudied winter season.

To address these hypotheses, we measured prokaryotic community composition and diversity, community respiration, and physicochemical water-column properties at stations inside and outside river plume influence. We correlated the relative abundances of individual populations across space with corresponding resource concentrations to determine if plume inputs influence the distributions of microbes. We then linked differentially distributed populations with known ecophysiological roles to predict how microbes may be using the river-borne carbon and nutrient compounds transported into the coastal ocean. Our observations and interpretations present predictions about the influence of river plume inputs on prokaryotic population distributions and bulk respiration rates along the Oregon coast, representing an important contribution to our understanding of the links between resources, environmental conditions, and prokaryotic community dynamics in the coastal ocean during the winter season.

2. MATERIALS AND METHODS

2.1. Sample collection

Two coastal transects were performed aboard the RV 'Oceanus': westward along the Newport Hydrographic Line beginning at the Yaquina River mouth (NH; 44.65° N) on 7 December 2016 and westward

along the Umpqua River Line beginning at the Umpqua River mouth (UR; 43.76° N) on 14 January 2017. Temperature, salinity, and total beam attenuation (a proxy for particle load) were monitored along each transect by continuous collection of surface water via the uncontaminated RV 'Oceanus' seawater intake (3–4 m below the waterline), which was routed through a Seabird thermosalinograph (SBE 45) and a Wetlabs C-star (650 nm, 25 cm pathlength). Seawater density was calculated from temperature, salinity, and pressure, using the 1980 equation of state (EOS-80). Using these real-time beam attenuation and density data, 3 stations were identified along each transect: (1) within the nearshore buoyant plume, (2) at a local particle maximum within the buoyant plume, and (3) on the shelf edge outside plume influence (see Table 1). We followed the approach of Mazzini et al. (2014) in defining the fresher, particle-rich discharge plume as inshore of the higher density front of the saltier offshore water (see Fig. 1).

At each of 3 sampling stations along the 2 transects (6 total stations), a CTD (Sea-bird) with a rosette of 24 Niskin bottles was deployed into surface water (~1 m). Three 0.5 l water samples were collected from separate CTD Niskin bottles into 3 collection carboys during each of the 6 deployments. Each collection carboy was rinsed thoroughly with water from its respective rosette Niskin bottle before being filled. Collection carboys were processed independently by filtering all 0.5 l through in-line 3 and 0.22 µm polyethersulfone (PES) membranes (Pall Corporation) to recover operationally defined particle-associated (PA) and free-living (FL) prokaryotic cell fractions, respectively. Collected biomass for each of the 36 samples (3 replicate collection carboys each filtered into 2 cell fractions at 3 stations along 2 transects) was stored in cryogenic tubes in an on-board liquid nitrogen dewar until return to the lab, where samples were frozen at −80°C until processing.

2.2. DNA extraction, 16S amplicon library construction, sequencing, and operational taxonomic unit clustering

DNA from filtered cells of all 36 samples was extracted independently using the CTAB protocol (Kieft et al. 2018). Extractions from 0.5 l samples yielded sufficient quantities of DNA for further analyses (~1–5 µg DNA). The v4 locus of the prokaryotic 16S rRNA gene was amplified and sequenced with Illumina MiSeq (Illumina) using the protocol described in Kozich et al. (2013). Single-step PCRs of 30 cycles were performed using ~50 ng of template DNA and AccuStart II PCR ToughMix Polymerase (QuantaBio) following manufacturer's instructions. The 515F (5′-GTG YCA GCM GCC GCG GTA A-3′) and 805rB (5′-GGA CTA CNV GGG TWT CTA AT-3′) primers were flanked by adapter regions, Nextera XT indices, pad sequences (to optimize melting temperature), and the anti-complementary linker sequences (Kozich et al. 2013). AMPure XP beads were used for amplicon purification, isolation, and cleanup.

Libraries of ~385 bp amplicons were normalized by concentration, pooled, and sequenced using an Illumina MiSeq v2 kit (251 bp, paired-end reads), generating an average of 12 603 paired-end reads per library. Libraries were demultiplexed and primer regions were stripped from sequences by the Center for Genome Research and Biocomputing at Oregon State University. The program USEARCH was used for paired-end read assembly, quality filtering, length trimming, and library normalization (Edgar 2010). First, paired-end reads were merged using 'fastq_mergepairs', with '-fastq_maxdiffs' set to 10 and '-fastq_pctid' set to 80 based on the long overlapping region design of paired-end sequencing amplicons. Resulting merged reads between 250 and 255 bp were retained and quality filtered using 'fastq_filter' with default parameters to remove any reads with a probability of a sequence error greater than zero. Merged, quality filtered reads from all libraries were then combined and clustered at 100% nucleotide identity using 'cluster_otus' with default parameters (Edgar 2013). The algorithm UNOISE was used to remove chimeras, discard singleton sequences, and create zero-radius operational taxonomic units (OTUs) based on the 16S v4 rRNA amplicon sequences. The OTU table was produced using the 'otutab' command and libraries were normalized using the 'otutab_norm' command with the '-sample_size' parameter set to 5000 (which rarefies samples to this read count by random subsampling without replacement) under the consideration that average unique sequence count was ~2600 library^{-1} and the algorithm suggests setting the '-sample_size' parameter at ~2× the average sequence count. This procedure yielded a per-sample normalized table of OTU counts clustered at 100% nucleotide identity. This method has been proposed to yield the most appropriate resolution for obtaining species-level clusters using the amplified 16S rRNA v4 region from environmental samples (Edgar 2018). Taxonomic classification of 16S amplicons was made with the 'sintax' command using the SILVA v4 region database

(v123). All 16S-amplicon sequences are available from NCBI (BioSample SAMN10869302, BioProject PRJNA520887, Accession numbers KCRC01000001–KCRC01002436).

2.3. Calculations of community composition, diversity, and assembly

Beta-diversity of prokaryotic communities was determined by calculating the weighted UniFrac distances of OTU relative abundance matrices using the function 'Unifrac()' from the R package 'phyloseq' (McMurdie & Holmes 2013). Beta-diversity was calculated and visualized using metric multidimensional scaling (principal coordinate analysis; PCoA) of the weighted UniFrac matrices. Significant differences in community composition across stations (longitudinally along each transect) for FL and PA microbes were determined by PERMANOVA using the 'adonis()' function from the R package 'vegan' (Oksanen et al. 2017). Significant similarity in the community composition between transects was determined with symmetric Procrustes transformation of the multidimensional weighted UniFrac shapes (PCoA axes) using the 'protest()' function from 'vegan'. Alpha-diversity was calculated as Faith's phylogenetic diversity (PD) and the net relatedness index (NRI) using functions from the R package 'picante' (Kembel et al. 2010). For NRI calculations, the 'richness' null model was used to calculate a separate null community relatedness for each of the 36 replicate samples, given that the identity and relative abundances of OTUs was hypothesized to differ along the zones of each transect.

2.4. Prokaryotic respiration measurements and cell counts

In order to estimate respiratory activity, decrease in dissolved oxygen (O_2) in sampled water over time was measured using the method described in Cory et al. (2013). For each sample, 9 exetainers (12 ml each) were washed thoroughly, filled slowly to the lip of the tube with collected water, and sealed with airtight stoppers. A total of 3 exetainer tubes of each sample set were then immediately amended to a final concentration of 1% $HgCl_2$ to halt biological activity and stored at 4°C until measurements were taken. The remaining 6 tubes were incubated in an onboard flow-through tank. Three tubes were incubated in the dark for 6 h and 3 for 12 hours, after which 1% $HgCl_2$ was added to each tube and all were stored at 4°C. O_2:argon ratios were measured for all samples (0, 6, and 12 h time points; 9 tubes sample^{-1}) using a membrane inlet mass spectrometer (MIMS; Bay Instruments and Pfeiffer Vacuum). Relative sample O_2 content and drawdown was calculated from these ratios by finding the slope (rate) of the oxygen loss over the 3 time points using dissolved gas ratio tables while controlling for machine drift with an offset parameter. Cell counts of FL microorganisms (samples pre-filtered at 3 µm to prevent line obstruction) were made using a Guava flow cytometer with a lower limit cutoff of 0.1 µm to remove count signals from non-biological debris.

2.5. Characterization of water chemistry

Samples for dissolved nutrient analyses were collected from each station by filtering seawater through a glass syringe fit with a Pall™ nylon 0.2 µm acrodisc into a clean 20 ml polycarbonate scintillation vial and stored at −20 °C until later analysis. In the laboratory, samples were thawed and run on a gas segmented Technicon Auto Analyzer II™. All dissolved nutrients were measured on a 5 cm flow cell, soluble reactive phosphate (hereafter PO_4^{3-}) was analyzed at 880 nm using the phosphomolybdic acid reduction method with hydrazine as the reductant (Gordon et al. 1993; adapted from Bernhardt & Wilhelms 1967); ammonium (NH_4^+) was measured at 640 nm and utilized the indophenol blue method as described by Gordon et al. (1993); nitrate + nitrite (NO_3^- and NO_2^-, respectively) concentrations were detected at 640 nm where NO_3^- is reduced to NO_2^- using a cadmium reduction coil as described by Wood et al. (1967); silicic acid (H_4SiO_4; hereafter Si), was measured at 660 nm using a method similar to that of the phosphate molybdic acid reduction, but using stannous chloride as a reductant (Gordon et al. 1993 adapted from Wood et al. 1967 and Atlas et al. 1971).

Particulate organic carbon (POC) and particulate nitrogen (PN) concentrations from splits of the same water samples were measured using the approach of Goñi et al. (2003, 2006). Briefly, known volumes (200–500 ml) of water from specific Niskin bottles in the CTD rosette were vacuum-filtered onto pre-combusted (400°C for 3 h) 13 mm glass fiber filters (Pall Life Science). At each location, similar volumes of filtered water were re-filtered through separate filters to determine the amounts of carbon and nitrogen associated with dissolved organic matter sorption onto filter fibers (e.g. Goñi et al. 2019). After filtration

was completed, all filters were folded into cleaned silver boats (Costech), placed in sample trays and kept frozen (−80°C) until analyses. Carbon and nitrogen analyses were performed using high-temperature combustion after exposing filters to concentrated acid fumes to remove carbonates as explained in Goñi et al. (2019). Daily multi-level calibrations were used to determine carbon and nitrogen contents in both samples and filter blanks, the latter of which were subtracted from the former to report POC and particulate organic nitrogen (PON) concentrations (µmol l^{-1}) after dividing by the volume filtered.

The dissimilarity in these nutrient profiles across stations was calculated by Euclidean distance matrices for each of the 2 transects. Significant differences in nutrient composition between samples in each transect were determined by PERMANOVA using the 'adonis()' function from 'vegan'. Significant similarity between transects was determined with symmetric Procrustes transformation of the multidimensional WU shape (PCoA axes) using the 'protest()' function from 'vegan'.

2.6. Environmental variable correlations with prokaryotic community composition

The 'bioenv()' function from 'vegan' was used to determine the combinatorial subset of biogeochemical and physical properties whose Euclidean distance matrix had the highest Pearson correlation with the weighted UniFrac distance matrix of combined OTU-level community composition across all samples (Oksanen et al. 2017). Given that the replicated biogeochemical concentrations and overall prokaryotic community composition were similar between the NH and UR transects (repeated Procrustes rotation squared m12 = 0.12, symmetric correlation = 0.94, $p < 0.001$), their environmental and prokaryotic data were combined to increase statistical power for correlation analyses, such that NH2 and UR3 were replicates for the nearshore plume, NH7 and UR9 for the mid-plume particle maximum, and NH25 and UR15 for the offshore shelf. Environmental variables were tested for normality using the Shapiro-Wilk test and Tukey-transformed to a normal distribution if Shapiro-Wilk $p < 0.05$ (Sokal & Rohlf 1995), and highly correlated variables ($\rho \geq 0.9$) were identified in a pair-wise manner using the 'findCorrelation()' function in the R package 'caret'; only one correlated variable was retained in subsequent analyses (Kuhn 2018). The subset of environmental variables with the highest correlation was considered the best combination of biogeochemical and physicochemical variables to explain the composition of prokaryotic communities (Oksanen et al. 2017). Correlations between environmental variables and individual OTUs were calculated using the program 'Calypso' with a false discovery rate (FDR) correction of p-values (Zakrzewski et al. 2017).

2.7. Indicator OTU calculations

The multi-level pattern analysis function of the R package 'indicspecies' ('multipatt()' with 999 permutations) was implemented to calculate indicator OTUs with differential abundances and occurrences across the combined NH and UR transect prokaryotic data. The purpose of this analysis was to determine populations with significant differences in distribution between zones along the transect; we inferred that these indicator groups represent other related taxa that increase or decrease gradually across space as a function of plume resources or conditions. An OTU population was considered to be an indicator and display strong preference for the habitat of a given sample if its 'multipatt()' specificity and fidelity were significantly associated ($p < 0.05$) with the sampling condition being tested.

3. RESULTS

3.1. River flow and coastal plume conditions

River discharge data from the United States Geological Survey in the 3 rivers adjacent to our transects (Alsea [Station ID: 14306500], Siuslaw [Station ID: 14307620], Umpqua [Station ID: 14321000], Yaquina is currently un-gauged) showed that discharge rates of Oregon Coastal Range rivers peaked shortly before the time of sampling on both the NH and UR transects (Fig. S1 in Supplement 1 at www.int-res.com/articles/suppl/a084p015_supp1.pdf). Continuous underway measurements of surface salinity (PSU) and beam attenuation (m^{-1}, a proxy for particle loads) showed evidence of a turbid, low-density water mass extending offshore from the coastline, encompassing Stns NH2 (nearshore-plume) and NH7 (mid-plume) in the NH transect and Stns UR3 (nearshore-plume) and UR9 (mid-plume) in the UR transect (Fig. 1). The plume structures were bounded offshore by a density and turbidity front at ~18 and ~10 nautical miles in the NH and UR transects, respectively; thus, Stns NH25 and UR15 were sampled to represent outside-plume

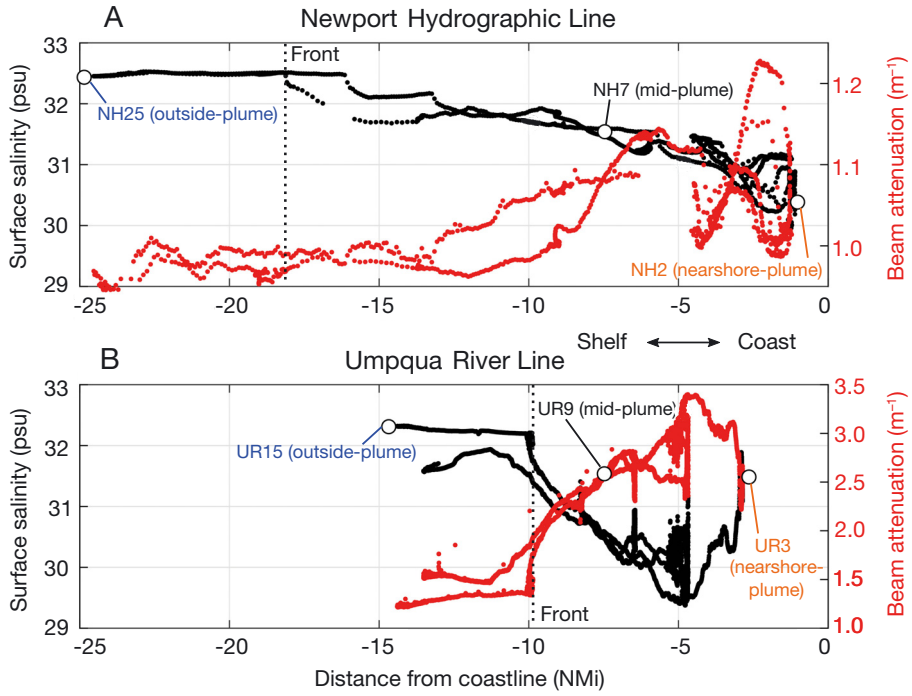

Fig. 1. Continuous underway data along the (A) Newport Hydrographic (NH; 44.65° N) and (B) Umpqua River (UR; 43.75° N) transects. Distance from coastline (*x*-axes) and salinity (left *y*-axes, black) are each on equivalent scales in both plots; beam attenuation (right *y*-axes, red) are on different scales. Red and black data points in each plot represent the out (coast-to-shelf) and in (shelf-to-coast) legs of each transect. Filled white circles: stations where CTD profiles were made; samples collected for this study are presented from Stns (A) NH2, NH7, and NH25 and (B) UR3, UR9, and UR15, which are detailed in the text and Table 1. Dotted vertical lines labeled 'Front' represent the defined boundary between plume (right of line) and non-plume (left of line) conditions. See Table 1 for station latitudes and condition details. All plotted data were collected from the ship's underway intake (~1 m)

conditions (Fig. 1). Notably, river discharge rates were much higher along the UR transect than along the NH transect, leading to absolute differences in bulk plume conditions between the 2 sampling lines, including lower water densities and higher beam attenuation values and a plume front nearer to shore at the UR compared to the NH transect (Fig. 1).

Inorganic nutrients (NO_3^-, NO_2^-, NH_4^+, PO_4^{3-}, and H_4SiO_4) in surface samples were in higher concentration at the nearshore- and mid-plume stations compared to outside-plume stations—for both the NH transect (PERMANOVA, $R^2 = 0.97$, $F = 137.2$, df = 5, p = 0.01) and the UR transect (PERMANOVA, $R^2 = 0.80$, $F = 16.4$, df = 5, p = 0.02). Stns NH2 and NH7 had similar inorganic nutrient concentrations (Tukey's HSD test, lower = –0.39; upper = 1.16; FDR-adjusted q = 0.24), which were higher than NH25 (NH2: 95% CI = 2.72–4.29, FDR-adjusted $q < 0.001$; NH7: 95% CI = 2.34–3.91, FDR-adjusted $q = 0.001$). Pairwise comparisons of all UR stations were significantly different in inorganic nutrient profiles ($p < 0.05$, Tukey's HSD statistics not shown), which generally decreased from UR3–UR15. Along the NH transect, NO_3^- and NO_2^- concentrations were most strongly associated with variation in nutrient profiles across the 3 stations (PERMANOVA explained variance of each term: NO_3^-: R^2 = 0.14, $F = 51.7$, p = 0.038; NO_2^-: $R^2 = 0.85$, $F = 312.6$, p = 0.015), while along the UR transect, PO_4^{3-} and NO_3^- significantly discriminated sampling stations (PERMANOVA explained variance of each term: PO_4^{3-}: $R^2 = 0.92$, $F = 356.8$, p = 0.004; NO_3^-: $R^2 = 0.06$, $F = 206.6$, p = 0.017). POC, PN, and beam attenuation were also higher in the plume stations than offshore (Table 1). Data detailing organic matter character (origin and composition) is currently in preparation (data not shown). PO_4^{3-}, NO_3^-, POC, and PON were in higher concentrations in the UR plume than the corresponding NH plume in accordance with higher river discharge rates, higher turbidity, and the strong density gradient along the UR transect; this pattern was not observed for Si, NO_2^-, or NH_4^+.

3.2. Respiration and cell abundance across the NH transect

The whole-water surface respiration rate in the mid-plume (Stn NH7) was ~3× higher than at NH2

Table 1. Physicochemical properties of sample water at each station. Sample ID and sample type are shown. Oxygen: oxygen saturation; Fluo.: fluorescence (FIECO-AFL); beam atten.: beam attenuation; PN: particulate organic nitrogen; POC: particulate organic carbon; Chl: chlorophyll *a*; PO_4: phosphate; NO_3: nitrate; SiO: silicate; NO_2: nitrite; NH_4: ammonium; Resp: respiration rate. Standard deviation of replicated measurements is shown in parentheses

	NH2 Nearshore-plume	NH7 Mid-plume	NH25 Outside-plume	UR3 Nearshore-plume	UR9 Mid-plume	UR15 Outside-plume
Latitude	44.65° N	44.65° N	44.65° N	43.76° N	43.76° N	43.76° N
Longitude	124.11° W	124.23° W	124.65° W	124.24° W	124.36° W	124.48° W
Date	7 Dec 2016	7 Dec 2016	7 Dec 2016	13 Jan 2017	14 Jan 2017	14 Jan 2017
Time (UTC)	14:18 h	10:48 h	02:24 h	21:01 h	00:47 h	03:52 h
Salinity (PSU)	30.42	31.52	32.48	31.40	31.50	32.29
Beam atten. (m^{-1})	1.06	1.09	0.82	2.56	2.61	1.21
Oxygen (µmol kg^{-1})	268.97	265.48	265.31	281.85	284.17	279.13
Fluo. (mg m^{-3})	0.86	1.11	1.20	0.89	1.28	1.35
Depth (m)	1.62	1.75	1.47	1.21	2.02	1.85
PN (µM)	0.68	0.78	0.46	0.85	0.89	0.50
POC (µM)	6.85	6.72	4.97	8.02	8.50	4.19
Chl (µg l^{-1})	1.17 (0.15)	1.15 (0.04)	1.96 (1.6)	1.17 (0.09)	1.21 (0.03)	0.97 (0.01)
PO_4 (µM)	0.73 (0.01)	0.66 (0.08)	0.68 (0.01)	1.13 (0.05)	0.98 (0)	0.91 (0)
NO_3 (µM)	5.71 (0.21)	5.62 (0.19)	2.87 (0)	10.21 (0.46)	9.2 (0.05)	7.22 (0.09)
SiO (µM)	70.74 (6.29)	29.76 (20.82)	49.89 (10.31)	64.9 (39.04)	53.9 (2.94)	33.51 (5.13)
NO_2 (µM)	0.33 (0.05)	0.36 (0.02)	0.22 (0.01)	0.35 (0)	0.27 (0)	0.25 (0)
NH_4 (µM)	1.14 (0.07)	0.94 (0)	0.65 (0.21)	2.43 (2.34)	0.28 (0.15)	0.19 (0.01)
Resp (µgC l^{-1} h^{-1})	2.76 (1.18)	6.47 (1.04)	2.49 (1.62)	NA	NA	NA

and NH25 (Table 1, Fig. 2). Respiration rates were measured along the UR transect, but could not be accurately recovered and reported due to methodological issues. Microbial cell counts (filtered to <3 µm) decreased from 2.0×10^6 to 1.0×10^6 to 0.78×10^6 m^{-1} at NH2, NH7, and NH25, respectively (Fig. 2); thus, estimated per-cell microbial respiration was also correspondingly highest at NH7.

3.3. Prokaryotic community composition and diversity

Prokaryotic communities across each transect were primarily differentiated from one another by lifestyle (FL and PA) and secondarily by collection station (Fig. 3). Given that the 2 lifestyles formed strongly significant groupings (PERMANOVA, $p < 0.001$ in both NH and UR) and were methodologically separated during sampling, the FL and PA communities were analyzed separately for all subsequent reported analyses. Both FL and PA communities significantly differed inside and outside the plume between Stns NH2, NH7, and NH25 (FL: PERMANOVA, $R^2 = 0.83$, $F = 12.5$, df = 7, $p = 0.011$; PA: $R^2 = 0.48$, $F = 1.9$, df = 6, $p = 0.040$) and between Stns UR3, UR9, and UR15 (FL: $R^2 = 0.56$, $F = 3.8$, df = 8, $p = 0.01$; PA: $R^2 = 0.67$, $F = 6.2$, df = 8, $p = 0.002$).

The PA fractions had higher phylogenetic alpha-diversity than their FL counterparts at all stations, but there was no significant spatial relationship of alpha-diversity across the plumes (Fig. 4A). More than half of all 16S rRNA amplicon sequences were annotated to 3 bacterial classes: *Alphaproteobacteria*, *Gammaproteobacteria*, and *Bacteroidetes* (Fig. S2 in Supplement 1). Other abundant OTUs were from *Archaea* and the bacterial phyla *Planctomycetes*, *Verrucomicrobia*, *Marinimicrobia*, and *Actinobacteria*.

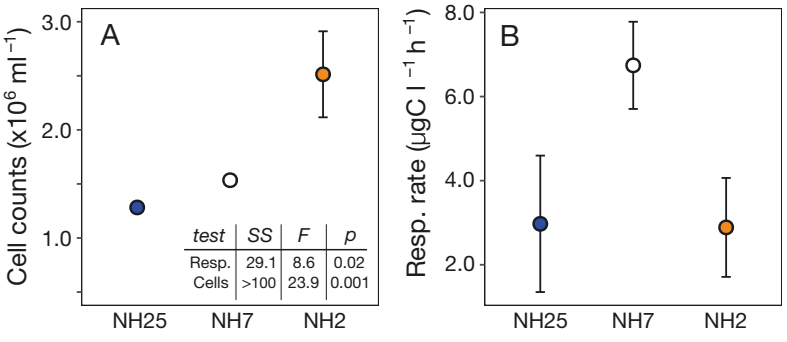

Fig. 2. Average (±SE) (A) cell counts and (B) respiration rates across the 3 stations on the Newport Hydrographic (NH) transect (measurements were not made on the Umpqua River transect). The Welch's *t*-test table shown in the inset of (A) compares the in-plume (NH2 and NH7) and out-plume (NH25) stations for (A) and (B)

Relatedness of populations within the community—determined by calculating the NRI, which measures the average branch length connecting 2 randomly chosen OTUs along the 16S rRNA tree—was greater at nearshore stations than at offshore shelf stations (Fig. 4B). Mean NRI of communities inside the plume was significantly higher (i.e. shorter branch lengths) than NRI of those outside the plume (Welch's *t*-test, $t = -4.1024$, df = 5.4499, $p = 0.0078$). It is important to note, however, that mean community NRI (replicate average) was not statistically significantly different from the null model (NRI quantile $p > 0.05$); thus, all communities sampled here are likely to be assembled primarily by stochastic mechanisms, rather than habitat filtering or competition, despite the spatial pattern of community NRI along the transects.

3.4. Relationships between biogeochemistry and community composition

Prokaryotic community composition data from the NH and UR were combined (after validation of similar spatial structure; see Section 2.6) in order to correlate composition with environmental conditions across space. Using the rank-based BIOENV procedure, FL community composition correlated best with the subset of temperature (negatively correlated with oxygen saturation), beam attenuation, and NO_2^- concentration (Spearman's $\rho = 0.55$), while the composition of the PA fraction correlated best with the subset of POC (positively correlated with PN), PO_4^{3-}, NO_3^-, and H_4SiO_4 concentrations (Spearman's $\rho = 0.35$).

Correlation calculations were implemented to identify the individual OTUs explaining these community-level patterns. A total of 264 OTUs were strongly correlated (absolute Pearson's $\rho > 0.4$, $p < 0.05$) with one of the identified environmental drivers of community composition differences between stations (Table S1 in Supplement 2 at www.int-res.com/articles/suppl/a084p015_supp2.xlsx). These populations ranged from relatively rare to dominant community members. Notably, the distributions of 3 predominately FL OTUs in the NO_2^--oxidizing group *Nitrospinaceae* were positively correlated with NO_3^- concentrations. Five *Comamonadaceae* OTUs were positively correlated with nutrient concentrations (NO_3^-, PO_4^{3-}) that were highest at the nearshore plume station, while no populations in this lineage were correlated with offshore conditions such as salinity (Table S1). Intriguingly, the *Bacteroidetes* lineage represented over 40% of populations that correlated with POC and PON concentrations but comprised <15% of OTUs correlated with salinity, temperature, and nutrients, while *Proteobacteria* populations showed the opposite trend of representation for these 2 sets of variables.

3.5. Population-level habitat preferences and indicator OTUs

The nearshore-plume (NH2, UR3), mid-plume (NH7, UR9), and outside-plume (NH25, UR15) stations were

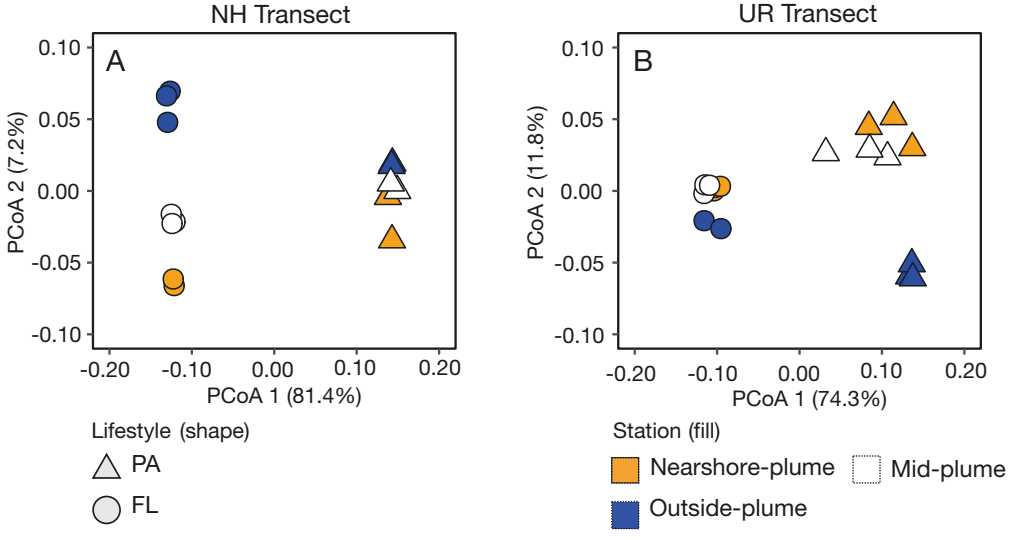

Fig. 3. Principal coordinate analysis (PCoA) plot of prokaryotic community structure as weighted UniFrac distances at stations along the (A) Newport Hydrographic (NH) and (B) Umpqua River (UR) transects. Nearshore-plume stations: NH2 (left) and UR3 (right); mid-plume stations: NH7 (left) and UR9 (right); outside-plume stations: NH25 (left) and UR15 (right). Variance explained by each PCoA axis is labeled by percentage next to each axis title. PA: particle-associated; FL: free-living

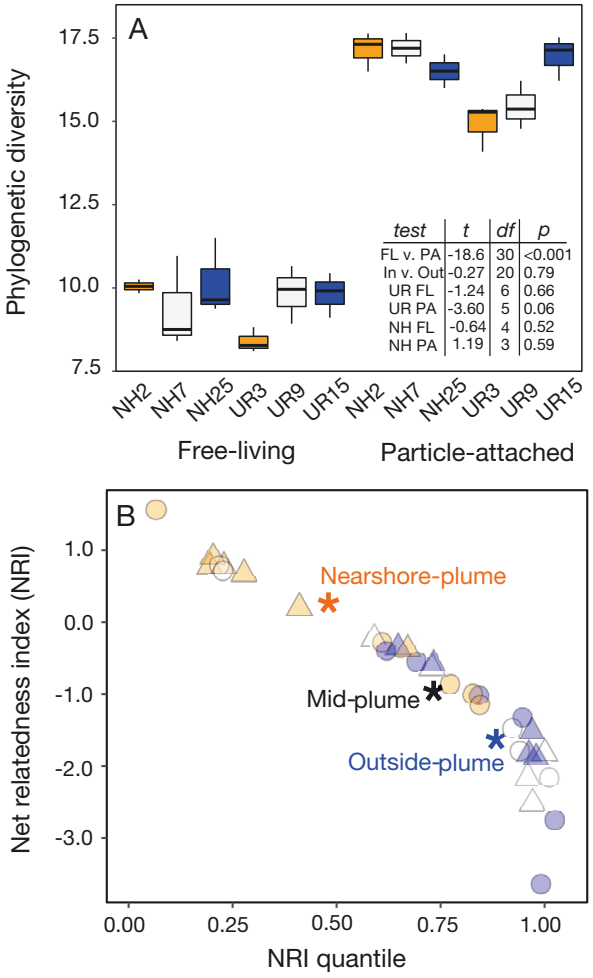

Fig. 4. (A) Faith's phylogenetic diversity; each box represents mean and first and third quartiles of replicates from a sampling station (Umpqua River, UR, or Newport Hydrographic, NH) within each lifestyle (free-living, FL or particle-attached, PA). Whiskers extend to the lowest and highest observations among the replicates. Inset table: paired *t*-tests between sampling groups to determine significant differences in alpha-diversity; FL vs. PA: columns 1–6 vs. 7–12; in vs. out: columns 1, 2, 4, 5, 7, 8, 10, 11 vs. 3, 6, 9, 12; UR FL: columns 4, 5 vs. 6; UR PA: columns 10, 11 vs. 12; NH FL: columns 1, 2 vs. 3; NH PA: columns 6, 7 vs. 8. (B) Net relatedness index (NRI): individual replicate samples are semi-transparent points (circles: FL; triangles: PA); zone averages are stars (nearshore-plume: NH2/UR3; mid-plume: NH7/UR9; outside-plume: NH25/UR15). *x*-axis: NRI quantile (p-value); *y*-axis: NRI value

distinguished by 64 (35 FL; 29 PA), 7 (3 FL; 4 PA), and 43 (34 FL; 9 PA) indicator OTUs, respectively. These indicator populations (Table S2 in Supplement 2) ranged in relative abundance from extremely rare to ~6% across samples and identified the specific OTUs that contributed to differences in community composition across the transects (Fig. 5).

The nearshore- and mid-plume indicators were comprised OTUs within the *Alphaproteobacterial* groups *Rhodobacteraceae* (7 total) and *Rhodospirillaceae* (4), and several populations of *Gammaproteobacteria* (i.e. *Coxiellaceae*: 2; *Porticoccaceae*: 1; *Psychromonadaceae*: 2; OMG182: 1; KI89A: 1; *Vibrionaceae*: 2; and *Chromatiales*: 1). *Bacteroidetes* OTUs that were indicators of plume samples were from NS1112 marine group (3), NS7 marine group (1), *Chitinophagaceae* (2), *Saprospiraceae* (1), *Porphyromonadaceae* (1), and *Marinilabiaceae* (1). Plume indicator OTUs from other lineages included populations of *Planctomycetaceae* (4), *Desulfobulbaceae* (4), *Methylophilaceae* (1), *Helicobacteraceae* (2), and *Campylobacteraceae* (1).

The offshore outside-plume station indicators were taxonomically distinct from those of the plume stations. *Alphaproteobacteria* OTUs from SAR11 (2), OCS116 (1), and *Rhodobacteraceae* (2) populations, along with *Gammaproteobacteria* OTUs in the SAR86 clade (2) and *Thiotrichales* (1), were indicator populations for non-plume conditions. There were relatively few *Bacteroidetes* indicators at the offshore station, limited to the PHOSHE51 *Sphingobacteriales* group (1) and *Flammeovirgaceae* (1). Several unclassified OTUs (4) and populations of *Cyanobacteria* (2), *Thermoplasmatales* (3), *Oligoflexaceae* (2), *Verrucomicrobiales* DEV007 (1), and SAR324 (1) were indicator OTUs outside the plume; almost all of these lineages were predominately found in the FL fraction and most had no representation as plume indicators.

4. DISCUSSION

Coastal microbial food webs are key drivers of biogeochemical cycles and facilitate bio-availability of resources for higher trophic levels (Fenchel 2008). In many coastal ecosystems, adjacent river plumes deliver freshwater and allochthonous substrates that can fundamentally shape the composition and diversity (Troussellier et al. 2002, Mason et al. 2016, Doherty et al. 2017, Thiele et al. 2017) and function (Albright 1983, Chin-Leo & Benner 1992, Lohrenz et al. 1999, Pakulski et al. 2000, Schlacher et al. 2009, Satinsky et al. 2014a) of microbial communities and the elemental cycles that they mediate (Gardner et al. 1996, Pakulski et al. 2000, Becquevort et al. 2002, Han et al. 2012).

In this work, we examined these ecological principles in plumes from 2 rivers along the central Oregon coast that export a majority of their annual organic carbon and nitrogen during winter seasons (Sin et al. 2007, Goñi et al. 2013). We observed several differ-

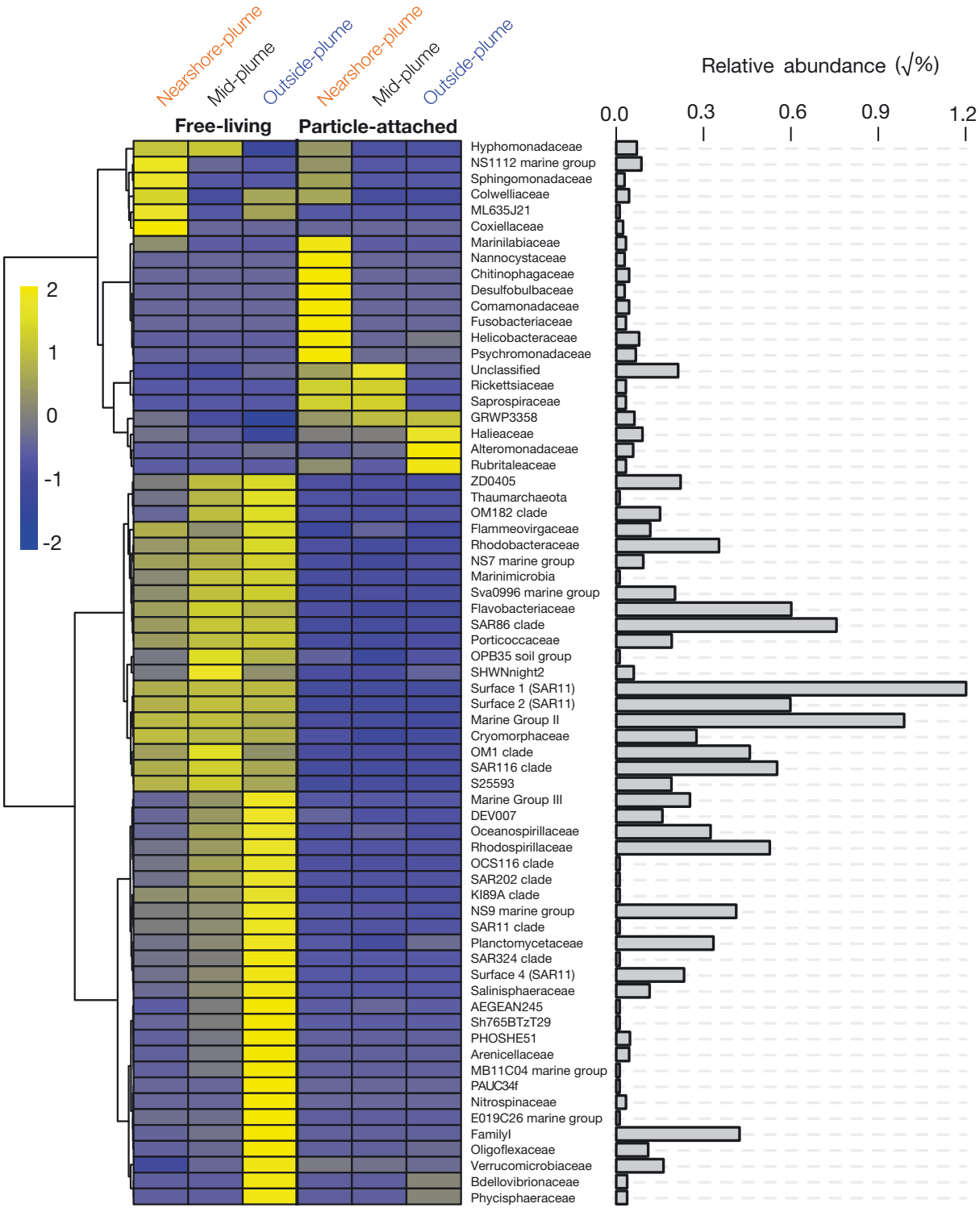

Fig. 5. Normalized relative abundances (*z*-score; yellow-blue scale-bar) of indicator operational taxonomic units (OTUs) grouped by Family (rows) across zone and lifestyle (columns). Newport Hydrographic (NH) and Umpqua River (UR) prokaryotic data sets were combined for indicator species analysis as detailed in Section 2.7. Row dendrogram shows similarity in indicator-OTU relative abundances across stations; heatmap columns are divided by free-living (left) and particle-attached (right) communities, then by nearshore-plume (NH2 and UR3; orange), mid-plume (NH7 and UR9; black), and outside-plume (NH25 and UR15; blue). Indicator-OTU affiliation with station and lifestyle, indicator score, p-value, and taxonomy can be found in Table S1. Horizontal barplot: square-root-transformed relative abundance (% of the total sequenced reads of each sample) for all the indicator OTUs grouped by Family

ences in coastal prokaryotic community composition between winter (our study) and non-winter (previous work) in this ecosystem, including a higher relative abundance of eukaryotic phytoplankton in the summer and of archaea in the winter, lower richness of rare *Gammaproteobacteria* in the summer, and a stronger distinction between FL and PA prokaryotic composition in the winter (Fortunato et al. 2012, 2013, Smith et al. 2013). In this discussion, we focus on how relationships between spatial distributions of prokaryotic populations and resource concentrations and physicochemical conditions influence our understanding of the fate of plume-derived resources on the Oregon coast and in other similar ecosystems.

4.1. Community diversity and relatedness

We observed significant spatial differences in prokaryotic phylogenetic relatedness but not in phylogenetic alpha-diversity across stations, though there was an overall higher diversity of PA compared to FL cells. Reports of river plume influence on coastal microbial diversity do not offer a consistent ecological framework for interpreting these results; for example, both enrichment (e.g. Mason et al. 2016) and depletion (e.g. Fortunato et al. 2012) of alpha-diversity in plume-influenced zones compared to adjacent habitats has been observed, and suspended particulate material (regardless of its origin) has been reported to host higher (DeLong et al. 1993, Kieft et al. 2018), similar (Hollibaugh et al. 2000), or lower (Mestre et al. 2018) alpha diversity in aquatic systems. Given these apparent discrepancies, we consider that diversity in 'transition zones' such as river plumes is likely to be strongly dependent on ecosystem context (Konopka et al. 2015). With respect to our study, Oregon coastal winter plumes are not short-lived, but rather accumulate via various physical forces into a thin and persistent seasonal buoyant current along the coastline (Mazzini et al. 2014). We speculate that the resulting long-lived gradients (such as those shown in Fig. 1) represent selective forces on certain prokaryotic clades, resulting in our observation of consistent alpha-diversity but distinct relatedness across space.

4.2. Lineage-specific patterns in distribution

Indicator and correlation analyses across cellular lifestyles and sampling stations suggested that many prokaryotic groups were influenced by or were interacting with resources derived from river plumes. Importantly, the general patterns of indicator population distributions we observed are in contrast to summer conditions in this ecosystem, where coastal surface ocean indicator taxa (off the Columbia River) were mainly comprised of heterotrophic prokaryotes that were associated with phytoplankton blooms and upwelling zones (see discussion of Fortunato et al. 2013). The strongest indicator groups for the nearshore-plume and mid-plume stations were composed of *Bacteroidetes* populations from *Chitinophagaceae*, *Marinilabiaceae*, and *Saprospiraceae*, and *Gammaproteobacteria* populations from *Coxiellaceae*, *Colwelliaceae*, OM182, and KI89A. Aquatic *Chitinophagaceae* isolates have a wide range of enzymatic activity on plant-derived biomass (Kishi et al. 2017), and members of *Colwelliaceae* can dramatically increase in abundance in marine surface water amended with terrestrially derived organic carbon and nitrogen compounds (Sipler et al. 2017). Some populations have been also found in close association with copepods and are hypothesized to derive nitrogen from these organisms (Moisander et al. 2015). OM182 and KI89A groups are considered oligotrophic gammaproteobacteria but form a separate clade from the OM60/NOR5, BD1-7, and SAR92 lineages (Spring et al. 2015); thus, their overrepresentation in the plume may be transient or suggest that they are not obligately oligotrophic and can survive and compete in plume conditions where nutrient conditions were higher relative to non-plume samples in our analysis. Indeed, KI89A have been observed to increase in relative abundance of a surface ocean community amended with inorganic nitrogen (Goldberg et al. 2017).

OTUs of sub-dominant lineages, such as the *Planctomycetales* and *Sphingobacteriales*, also had several FL indicators within plume samples, and members of these groups have been predicted to have copiotrophic life strategies based on their genome features (Lauro et al. 2009). *Desulfobulbaceae*, *Vibrionaceae*, and *Campylobacterales* populations were commonly indicator species for the PA fraction of plume samples. These groups represent lineages of well-established coastal ocean particle colonizers (Fortunato et al. 2013, Smith et al. 2013, Yawata et al. 2014, Datta et al. 2016, Duret et al. 2019) and are resident taxa on suspended particles of the estuary adjacent to the NH Line (Kieft et al. 2018). In addition, *Campylobacterales* taxa have been recently observed to increase in relative abundance in coastal water amended with terrestrial organic material (Sipler et al. 2017) or complex polysaccharides (Reintjes et al. 2019).

Notably, most of these indicator groups had little or no representation as indicators outside the plume stations, where indicator OTUs were mostly composed of different family-level lineages (e.g. *Flammeovirgaceae*, SAR86 clade, *Oligoflexaceae*, and *Thiotrichales*). The potential specialized ecological roles of these plume-specific populations remain unknown but, based on our observations, it is reasonable to hypothesize that some of the groups representative of conditions at plume stations may be participating in the turnover of plume-derived dissolved and particulate carbon and nutrient resources, ultimately influencing the fate of the terrestrially derived organic matter entering the coastal ocean (Bianchi 2011).

4.3. Relationships between respiratory activity, plume conditions, and population distribution

Along the NH line in our study, oxygen drawdown rate (used as a proxy for organic carbon loss via biological oxidation) at Stn NH7 exceeded that of the nearshore-plume and offshore shelf waters by ~3-fold (Fig. 2). Given that there were no obvious prokaryotic populations more dominant in the NH7 samples than in the 2 other stations, interactions between community members and/or with the environment or unmeasured abiotic features may be responsible for the increased heterotrophy in this zone. Regardless, our findings support the emerging understanding that habitats along strong biogeochemical continua provide unique sets of niches (e.g. Satinsky et al. 2014b, Benner & Amon 2015, Mestre et al. 2017), often supporting spatially distinct elemental fluxes or turnover processes (Stocker 2012, Suter et al. 2018). For example, a zone near the density front of the Columbia River plume has been shown to support a distinct prokaryotic community and higher total RNA concentrations and leucine incorporation rates than in the estuary or on the shelf (Smith et al. 2010). Given that carbon and nutrient concentrations are often higher in buoyant plume water (Tian et al. 1993, Lohrenz et al. 1999, Geyer et al. 2004) and are linked to plume productivity (Klinkhammer et al. 1997), sampling efforts to estimate system-level processes (e.g. net trophic status) in coastal zones with significant river plume inputs should define physical and chemical gradients created by plumes as a way to collect relevant samples from inside, at strong transition zones (e.g. particle maxima), and outside of plume-influenced areas.

5. CONCLUSIONS

Linking population relative abundance with participation in ecological functions, such as resource cycling, continues to be a widely discussed topic in microbial ecology (Bier et al. 2015), and results should always be considered in the context of the environment under investigation. For example, the connectivity between terrestrial and marine ecosystems during the plume conditions captured in our study could lead to observations of 'tourist taxa' that may have little impact on ecosystem function (e.g. Lee et al. 2017). Although this phenomenon is likely present to some extent in our data set, the populations discussed in more detail were corroborated as native coastal organisms by examining community compositions reported from similar coastal environments (e.g. Smith et al. 2010, 2013, Fortunato et al. 2013). A related mechanism not captured with detailed resolution in this exploratory data set is dispersal and dilution of plume-derived particulate and dissolved material over time and space upon entering the coastal ocean; therefore, the biological turnover and transformation of resources transported by the plume are likely also being catalyzed by non-plume marine microorganisms (i.e. at different depths or offshore outside the apparent plume-influenced zone). Despite these important considerations, this study provides the first insights into Oregon coast prokaryotic communities in the context of winter river plumes, which are hypothesized to be a major source of carbon and nutrients subsidizing the activity of the winter food web in this ecosystem. Future research should extend this effort with higher resolution sampling across space and time to verify our observations, as well as conduct experiments to test hypotheses of plume resource turnover by specific taxonomic groups put forward in this work. Taken together, we propose a scenario in which allochthonous particulate and dissolved resources delivered by plumes structure a specific assemblage of prokaryotes whose metabolic activity helps to fuel winter ecosystem productivity.

Acknowledgements. We are grateful to the captain and crew of the RV 'Oceanus' for enabling the 2 sampling expeditions. Dr. Steve Giovannoni at Oregon State University allowed us to use his laboratory Guava Flow Cytometer and Eric Moore assisted in cell count acquisition. This work was supported in part by the National Science Foundation (OCE-1642295 to M.A.G. and A.E.W.) and by the Margaret and Charles Black Scholarship through the Department of Microbiology at Oregon State University.

LITERATURE CITED

Albright LJ (1983) Influence of river-ocean plumes upon bacterioplankton production of the Strait of Georgia, British Columbia. Mar Ecol Prog Ser 12:107–113

Alonso-Sáez L, Gasol JM (2007) Seasonal variations in the contributions of different bacterial groups to the uptake of low-molecular-weight compounds in northwestern Mediterranean coastal waters. Appl Environ Microbiol 73:3528–3535

Atlas EL, Hager SL, Gordon LI, Park PK (1971) A practical manual for use of the Technicon Autoanalyzer in seawater nutrient analyses; revised. Technical Report No. 215, Reference 71-22. Oregon State University, Department of Oceanography, Corvallis, OR

Bauer JE, Cai WJ, Raymond PA, Bianchi TS, Hopkinson CS, Regnier PAG (2013) The changing carbon cycle of the coastal ocean. Nature 504:61–70

Becquevort S, Bouvier T, Lancelot C, Cauwet G, Deliat G, Egorov VN, Popovichev VN (2002) The seasonal modulation of organic matter utilization by bacteria in the Danube–Black Sea mixing zone. Estuar Coast Shelf Sci 54:337–354

Benner R, Amon RMW (2015) The size-reactivity continuum of major bioelements in the ocean. Annu Rev Mar Sci 7: 185–205

Bernhardt H, Wilhelms A (1967) The continuous determination of low level iron, soluble phosphate and total phosphate with the AutoAnalyzer. In: Automation in analytical chemistry: Technicon Symposia, Vol 1. Mediad, White Plains, NY, p 385–389

Bianchi TS (2011) The role of terrestrially derived organic carbon in the coastal ocean: a changing paradigm and the priming effect. Proc Natl Acad Sci USA 108:19473–19481

Bier RL, Bernhardt ES, Boot CM, Graham EB and others (2015) Linking microbial community structure and microbial processes: an empirical and conceptual overview. FEMS Microbiol Ecol 91:fiv113

Brown CA, Ozretich RJ (2009) Coupling between the coastal ocean and Yaquina Bay, Oregon: importance of oceanic inputs relative to other nitrogen sources. Estuaries Coasts 32:219–237

Cai WJ (2003) Riverine inorganic carbon flux and rate of biological uptake in the Mississippi River plume. Geophys Res Lett 30:1032

Capone DG, Hutchins DA (2013) Microbial biogeochemistry of coastal upwelling regimes in a changing ocean. Nat Geosci 6:711–717

Chase Z, Strutton PG, Hales B (2007) Iron links river runoff and shelf width to phytoplankton biomass along the US West Coast. Geophys Res Lett 34:L04607

Checkley DM, Barth JA (2009) Patterns and processes in the California Current System. Prog Oceanogr 83:49–64

Chin-Leo G, Benner R (1992) Enhanced bacterioplankton production and respiration at intermediate salinities in the Mississippi River plume. Mar Ecol Prog Ser 87: 87–103

Cory RM, Crump BC, Dobkowski JA, Kling GW (2013) Surface exposure to sunlight stimulates CO_2 release from permafrost soil carbon in the Arctic. Proc Natl Acad Sci USA 110:3429–3434

Datta MS, Sliwerska E, Gore J, Polz MF, Cordero OX (2016) Microbial interactions lead to rapid micro-scale successions on model marine particles. Nat Commun 7:11965

DeLong EF, Franks DG, Alldredge AL (1993) Phylogenetic diversity of aggregate-attached vs. free-living marine bacterial assemblages. Limnol Oceanogr 38:924–934

Doherty M, Yager PL, Moran MA, Coles VJ and others (2017) Bacterial biogeography across the Amazon River-ocean continuum. Front Microbiol 8:882

Duret MT, Lampitt RS, Lam P (2019) Prokaryotic niche partitioning between suspended and sinking marine particles. Environ Microbiol Rep 11:386–400

Edgar RC (2010) Search and clustering orders of magnitude faster than BLAST. Bioinformatics 26:2460–2461

Edgar RC (2013) UPARSE: highly accurate OTU sequences from microbial amplicon reads. Nat Methods 10:996–998

Edgar RC (2018) Updating the 97% identity threshold for 16SRNA OTUs. Bioinformatics 34:2371–2375

Evans W, Hales B, Strutton PG (2011) Seasonal cycle of surface ocean pCO_2 on the Oregon shelf. J Geophys Res 116:C05012

Fenchel T (2008) The microbial loop — 25 years later. J Exp Mar Biol Ecol 366:99–103

Fortunato CS, Herfort L, Zuber P, Baptista AM, Crump BC (2012) Spatial variability overwhelms seasonal patterns in bacterioplankton communities across a river to ocean gradient. ISME J 6:554–563

Fortunato CS, Eiler A, Herfort L, Needoba JA, Peterson TD, Crump BC (2013) Determining indicator taxa across spatial and seasonal gradients in the Columbia River coastal margin. ISME J 7:1899–1911

Gardner WS, Benner R, Amon RMW, Cotner JB Jr, Cavaletto JF, Johnson JR (1996) Effects of high-molecular-weight dissolved organic matter on nitrogen dynamics in the Mississippi River plume. Mar Ecol Prog Ser 133:287–297

Geyer WR, Hill PS, Kineke GC (2004) The transport, transformation and dispersal of sediment by buoyant coastal flows. Cont Shelf Res 24:927–949

Ghiglione JF, Murray AE (2012) Pronounced summer to winter differences and higher wintertime richness in coastal Antarctic marine bacterioplankton. Environ Microbiol 14:617–629

Goldberg SJ, Nelson CE, Viviani DA, Shulse CN, Church MJ (2017) Cascading influence of inorganic nitrogen sources on DOM production, composition, lability and microbial community structure in the open ocean. Environ Microbiol 19:3450–3464

Goñi MA, Teixeira MJ, Perkey DW (2003) Sources and distribution of organic matter in a river-dominated estuary (Winyah Bay, SC, USA). Estuar Coast Shelf Sci 57: 1023–1048

Goñi MA, Gordon ES, Monacci NM, Clinton R, Gisewhite R, Allison MA, Kineke G (2006) The effect of Hurricane Lili on the distribution of organic matter along the inner Louisiana shelf (Gulf of Mexico, USA). Cont Shelf Res 26: 2260–2280

Goñi MA, Hatten JA, Wheatcroft RA, Borgeld JC (2013) Particulate organic matter export by two contrasting small mountainous rivers from the Pacific Northwest, USA. J Geophys Res Biogeosciences 118:112–134

Goñi MA, Corvi ER, Welch KA, Buktenica M, Lebon K, Alleau Y, Juranek LW (2019) Particulate organic matter distributions in surface waters of the Pacific Arctic shelf during the late summer and fall season. Mar Chem 211:75–93

González N, Anadón R, Viesca L (2003) Carbon flux through the microbial community in a temperate sea during summer: role of bacterial metabolism. Aquat Microb Ecol 33: 117–126

Gordon LI, Jennings JC, Ross AA, Krest JM (1993) A suggested protocol for continuous flow automated analysis of seawater nutrients (phosphate, nitrate, nitrite and silicic acid) in the WOCE Hydrographic Program and the Joint Global Ocean Fluxes Study. WOCE Hydrographic Program Office Methods Manual WHPO 91-1

Guenet B, Danger M, Abbadie L, Lacroix G (2010) Priming effect: bridging the gap between terrestrial and aquatic ecology. Ecology 91:2850–2861

Han A, Dai M, Kao SJ, Gan J and others (2012) Nutrient dynamics and biological consumption in a large continental shelf system under the influence of both a river plume and coastal upwelling. Limnol Oceanogr 57:486–502

Hastings RH, Goñi MA, Wheatcroft RA, Borgeld JC (2012) A terrestrial organic matter depocenter on a high-energy margin: the Umpqua River system, Oregon. Cont Shelf Res 39–40:78–91

Hollibaugh JT, Wong PS, Murrell MC (2000) Similarity of particle-associated and free-living bacterial communities in northern San Francisco Bay, California. Aquat Microb Ecol 21:103–114

Horner-Devine AR, Hetland RD, MacDonald DG (2015) Mixing and transport in coastal river plumes. Annu Rev Fluid Mech 47:569–594

Kembel SW, Cowan PD, Helmus MR, Cornwell WK and others (2010) Picante: R tools for integrating phylogenies and ecology. Bioinformatics 26:1463–1464

Kieft B, Li Z, Bryson S, Crump BC and others (2018) Microbial community structure–function relationships in Yaquina Bay Estuary reveal spatially distinct carbon and nitrogen cycling capacities. Front Microbiol 9: 1282

Kishi LT, Lopes EM, Fernandes CC, Fernandes GC, Sacco LP, Alves LMC, Lemos EGM (2017) Draft genome sequence of a *Chitinophaga* strain isolated from a lignocellulose biomass-degrading consortium. Genome Announc 5:e01056-16

Klinkhammer GP, Chin CS, Wilson C, Rudnicki MD, German CR (1997) Distributions of dissolved manganese and fluorescent dissolved organic matter in the Columbia River estuary and plume as determined by in situ measurement. Mar Chem 56:1–14

Konopka A, Lindemann S, Fredrickson J (2015) Dynamics in microbial communities: unraveling mechanisms to identify principles. ISME J 9:1488–1495

Kozich JJ, Westcott SL, Baxter NT, Highlander SK, Schloss PD (2013) Development of a dual-index sequencing strategy and curation pipeline for analyzing amplicon sequence data on the MiSeq Illumina sequencing platform. Appl Environ Microbiol 79:5112–5120

Kuhn M (2018) caret: classification and regression training. R package version 6.0-79. https://CRAN.R-project.org/package=caret

Lauro FM, McDougald D, Thomas T, Williams TJ and others (2009) The genomic basis of trophic strategy in marine bacteria. Proc Natl Acad Sci USA 106:15527–15533

Lee E, Shin D, Hyun SP, Ko KS and others (2017) Periodic change in coastal microbial community structure associated with submarine groundwater discharge and tidal fluctuation. Limnol Oceanogr 62:437–451

Lohrenz SE, Fahnenstiel GL, Redalje DG, Lang GA, Dagg MJ, Whitledge TE, Dortch Q (1999) Nutrients, irradiance, and mixing as factors regulating primary production in coastal waters impacted by the Mississippi River plume. Cont Shelf Res 19:1113–1141

Mason OU, Canter EJ, Gillies LE, Paisie TK, Roberts BJ (2016) Mississippi River plume enriches microbial diversity in the northern Gulf of Mexico. Front Microbiol 7:1048

Mazzini PLF, Barth JA, Shearman RK, Erofeev A (2014) Buoyancy-driven coastal currents off Oregon during fall and winter. J Phys Oceanogr 44:2854–2876

McMurdie PJ, Holmes S (2014) Shiny-phyloseq: web application for interactive microbiome analysis with provenance tracking. Bioinformatics 31:282–283

Mestre M, Borrull E, Sala MM, Gasol JM (2017) Patterns of bacterial diversity in the marine planktonic particulate matter continuum. ISME J 11:999–1010

Mestre M, Ruiz-González C, Logares R, Duarte CM, Gasol JM, Sala MM (2018) Sinking particles promote vertical connectivity in the ocean microbiome. Proc Natl Acad Sci USA 115:E6799–E6807

Moisander PH, Sexton AD, Daley MC (2015) Stable associations masked by temporal variability in the marine copepod microbiome. PLOS ONE 10:e0138967

Montero P, Daneri G, Cuevas LA, González HE, Jacob B, Lizárraga L, Menschel E (2007) Productivity cycles in the coastal upwelling area off Concepción: the importance of diatoms and bacterioplankton in the organic carbon flux. Prog Oceanogr 75:518–530

Nieblas AE, Sloyan BM, Hobday AJ, Coleman R, Richardsone AJ (2009) Variability of biological production in low wind-forced regional upwelling systems: a case study off southeastern Australia. Limnol Oceanogr 54:1548–1558

Oksanen J, Blanchet FG, Friendly M, Kindt R and others (2017) vegan: community ecology package. R package version 2.4-6. https://CRAN.R-project.org/package=vegan

Pakulski JD, Benner R, Amon R, Eadie B, Whitledge T (1995) Community metabolism and nutrient cycling in the Mississippi River plume: evidence for intense nitrification at intermediate salinities. Mar Ecol Prog Ser 117:207–218

Pakulski JD, Benner R, Whitledge T, Amon R and others (2000) Microbial metabolism and nutrient cycling in the Mississippi and Atchafalaya River plumes. Estuar Coast Shelf Sci 50:173–184

Reintjes G, Arnosti C, Fuchs B, Amann R (2019) Selfish, sharing and scavenging bacteria in the Atlantic Ocean: a biogeographical study of bacterial substrate utilisation. ISME J 13:1119–1132

Saldías GS, Sobarzo M, Largier J, Moffat C, Letelier R (2012) Seasonal variability of turbid river plumes off central Chile based on high-resolution MODIS imagery. Remote Sens Environ 123:220–233

Satinsky BM, Crump BC, Smith CB, Sharma S and others (2014a) Microspatial gene expression patterns in the Amazon River plume. Proc Natl Acad Sci USA 111: 11085–11090

Satinsky BM, Zielinski BL, Doherty M, Smith CB and others (2014b) The Amazon continuum dataset: quantitative metagenomic and metatranscriptomic inventories of the Amazon River plume, June 2010. Microbiome 2:17

Schlacher TA, Connolly RM, Skillington AJ, Gaston TF (2009) Can export of organic matter from estuaries support zooplankton in nearshore, marine plumes? Aquat Ecol 43:383–393

Sigleo AC, Frick WE (2007) Seasonal variations in river discharge and nutrient export to a Northeastern Pacific estuary. Estuar Coast Shelf Sci 73:368–378

Sin Y, Sigleo AC, Song E (2007) Nutrient fluxes in the microalgal-dominated intertidal regions of the lower Yaquina Estuary, Oregon (USA). Northwest Sci 81:50–61

Sipler RE, Kellogg CTE, Connelly TL, Roberts QN, Yager PL, Bronk DA (2017) Microbial community response to terrestrially derived dissolved organic matter in the coastal Arctic. Front Microbiol 8:1018

Smith MW, Herfort L, Tyrol K, Suciu D and others (2010) Seasonal changes in bacterial and archaeal gene expression patterns across salinity gradients in the Columbia River coastal margin. PLOS ONE 5:e13312

Smith MW, Zeigler Allen L, Allen AE, Herfort L, Simon HM (2013) Contrasting genomic properties of free-living and particle-attached microbial assemblages within a coastal ecosystem. Front Microbiol 4:120

Sokal RR, Rohlf FJ (1995) Biometry the principles and practice of statistics in biological research, 3rd edn. WH Freeman, New York, NY

Sowell SM, Abraham PE, Shah M, Verberkmoes NC, Smith DP, Barofsky DF, Giovannoni SJ (2011) Environmental proteomics of microbial plankton in a highly productive coastal upwelling system. ISME J 5:856–865

Spring S, Scheuner C, Göker M, Klenk HP (2015) A taxonomic framework for emerging groups of ecologically important marine gammaproteobacteria based on the reconstruction of evolutionary relationships using genome-scale data. Front Microbiol 6:382

Stedmon CA, Thomas DN, Granskog M, Kaartokallio H, Papadimitriou S, Kuosa H (2007) Characteristics of dissolved organic matter in Baltic coastal sea ice: Allochthonous or autochthonous origins? Environ Sci Technol 41: 7273–7279

Stocker R (2012) Marine microbes see a sea of gradients. Science 338:628–633

Suter EA, Pachiadaki M, Taylor GT, Astor Y, Edgcomb VP (2018) Free-living chemoautotrophic and particle-attached heterotrophic prokaryotes dominate microbial assemblages along a pelagic redox gradient. Environ Microbiol 20:693–712

Thiele S, Richter M, Balestra C, Glöckner FO, Casotti R (2017) Taxonomic and functional diversity of a coastal planktonic bacterial community in a river-influenced marine area. Mar Genomics 32:61–69

Tian RC, Hu FX, Martin JM (1993) Summer nutrient fronts in the Changjiang (Yantze River) estuary. Estuar Coast Shelf Sci 37:27–41

Troussellier M, Schäfer H, Batailler N, Bernard L and others (2002) Bacterial activity and genetic richness along an estuarine gradient (Rhone River plume, France). Aquat Microb Ecol 28:13–24

Vargas CA, Martínez RA, Cuevas LA, Pavez MA (2007) The relative importance of microbial and classical food webs in a highly productive coastal upwelling area. Limnol Oceanogr 52:1495–1510

Wetz MS, Hales B, Chase Z, Wheeler PA, Whitney MM (2006) Riverine input of macronutrients, iron, and organic matter to the coastal ocean off Oregon, USA, during the winter. Limnol Oceanogr 51:2221–2231

Woebken D, Teeling H, Wecker P, Dumitriu A and others (2007) Fosmids of novel marine *Planctomycetes* from the Namibian and Oregon coast upwelling systems and their cross-comparison with planctomycete genomes. ISME J 1:419–435

Wood ED, Armstrong FAJ, Richards FA (1967) Determination of nitrate in sea water by cadmium-copper reduction to nitrite. J Mar Biol Assoc UK 47:23–31

Yawata Y, Cordero OX, Menolascina F, Hehemann JH, Polz MF, Stocker R (2014) Competition-dispersal tradeoff ecologically differentiates recently speciated marine bacterioplankton populations. Proc Natl Acad Sci USA 111: 5622–5627

Zakrzewski M, Proietti C, Ellis JJ, Hasan S, Brion MJ, Berger B, Krause L (2017) Calypso: a user-friendly web-server for mining and visualizing microbiome–environment interactions. Bioinformatics 33:782–783

Editorial responsibility: Eva Lindström, Uppsala, Sweden

Submitted: April 5, 2019; Accepted: September 30, 2019
Proofs received from author(s): December 20, 2019